

# Stability Boundaries of Tetrahydrofuran + Water System

Takashi Makino, Takeshi Sugahara, and Kazunari Ohgaki\*

Division of Chemical Engineering, Graduate School of Engineering Science, Osaka University, Toyonaka, Osaka 560-8531, Japan

Phase equilibria for the tetrahydrofuran + water system below atmospheric pressure were investigated in a temperature range from 272 K to 278 K. The three-phase (structure-II hydrate + aqueous solution + gas) equilibrium curve has a maximum temperature at  $277.45 \pm 0.02$  K and a pressure of  $4.9 \pm 0.1$  kPa. At this condition, the equilibrium tetrahydrofuran composition of aqueous solution is equal to the stoichiometric ratio of tetrahydrofuran hydrate (structure-II). The tetrahydrofuran hydrate does not coexist with the gas phase beyond 277.45 K. The four-phase (structure-II hydrate + aqueous solution + ice Ih + gas) equilibrium point exists at  $272.06 \pm 0.02$  K and  $1.1 \pm 0.1$  kPa, and the equilibrium tetrahydrofuran mole fraction of aqueous solution is  $0.0106 \pm 0.0002$ .

## Introduction

Tetrahydrofuran (THF) is one of the most well-investigated guest species in the clathrate hydrate systems, mainly because THF as an additive to other gas hydrate systems is able to reduce the equilibrium pressure dramatically. Therefore, it makes it possible to treat gas hydrates under mild pressure conditions. The recent study has reported that the molecular hydrogen is enclathrated in structure-II (s-II) with cooperative assistance of THF at ambient pressure and temperature conditions.<sup>1,2</sup> The stability boundaries of the THF hydrate system are also very important in light of hydrogen storage materials.

In a low-pressure region, the pure THF hydrate is regarded as s-II hydrate, which is constructed from 16 pentagonal dodecahedron hydrate cages (S-cage), 8 hexakaidecahedron hydrate cages (L-cage), and 136 H<sub>2</sub>O molecules in the unit cell.<sup>3,4</sup> The THF molecules are able to occupy the L-cage only, as the S-cage is vacant because of its large molecular size. The chemical formula for the ideal hydration is then given as THF·17H<sub>2</sub>O.<sup>5</sup>

The phase behavior for THF hydrate system has not been investigated in detail, although the stability boundaries at a high-pressure region have been reported in ref 6 and ref 7.

The most characteristic point in the THF hydrate system is the existence of a univariant two-phase (hydrate + aqueous solution) coexistence curve. The composition of aqueous solution in equilibrium with the s-II THF hydrate is equal to the mole stoichiometric ratio of s-II THF hydrate (1:17). The two-phase equilibrium curve is the univariant property in the temperature–pressure projection, although it does not exactly correspond to the three-phase coexistence in the binary system.

The purpose of the present study is to describe the phase behavior or stability boundaries in the low-pressure region (below atmospheric pressure condition). Below atmospheric pressure, the univariant two-phase coexistence curve and two three-phase (hydrate + aqueous solution + gas) coexistence curves are the subject of the present investigation. We speculate from the literature<sup>8–11</sup> that these three

curves converge around 277 K. The phase–equilibrium curves were determined using an ordinary method.

## Experimental Section

**Materials.** THF (purity: >99.9 %) was purchased from Merck Co., Ltd. The distilled water was purchased from Yashima Pure Chemical Co., Ltd. All of them were used without further purification.

**Apparatus and Procedure.** The phase behavior was observed with an ordinary static method. A glass cell having an inner volume of  $\approx 30$  cm<sup>3</sup> was immersed in a temperature-controlled water bath. The equilibrium temperature was measured using a thermistor probe (TAKARA D632) within a reproducibility of 0.02 K. A strain pressure gauge (Valcom VHR3, calibrated with the saturated vapor pressure of pure THF) was used for determining the equilibrium pressure with an estimated maximum uncertainty of 0.1 kPa.

Aqueous solutions of different THF concentrations, listed in Table 1, were prepared including the stoichiometric solution (the THF mole fraction of stoichiometric solution is 0.0556 (=1/18) for s-II hydrate). The electric balance (Shimadzu BL-220H) was used for preparing the solutions, and the mole fraction of the aqueous solution was determined with an estimated maximum uncertainty of 0.0001. Each mixture introduced into the glass cell was sufficiently degassed by a freezing method. Then, the melted contents were agitated by use of magnetic stirrer for establishing the phase-equilibrium state. Under the three-phase coexistence conditions, the phase-equilibrium curve (pressure–temperature relation) is essentially independent of the composition of mixture from the Gibbs phase rule. In this case, the mole fraction of aqueous solution in equilibrium was not determined because the initial concentration in aqueous solution was changed by THF hydrate or ice Ih formation (except for the stoichiometric solution in which the concentration never changes regardless of THF hydrate formation). To obtain the pressure–temperature relation including equilibrium composition of aqueous solution, we have to increase the system temperature very gradually and establish gas–liquid equilibrium in the presence of a negligibly small amount of THF hydrate or ice Ih. That is, the three-phase coexisting relation including equilibrium

\* To whom correspondence should be addressed. Phone: +81-6-6850-6290. Fax: +81-6-6850-6290. E-mail: ohgaki@cheng.es.osaka-u.ac.jp.

**Table 1. Equilibrium Pressure–Temperature–Composition Relation for THF + Water System below the Atmospheric Pressure Condition**

$x_{\text{THF}}$	$T/\text{K}$	$p/\text{kPa}$
	$\text{S}_1\text{L}_1\text{G}$	
0.0020	273.00	0.7
0.0050	272.73	0.9
0.0089	272.31	1.0
	$\text{H}_{\text{II}}\text{S}_1\text{L}_1\text{G}$	
0.0106	272.06	1.1
	$\text{H}_{\text{II}}(\text{L}_1 \text{ or } \text{L}_2)\text{G}$	
0.0113	272.27	1.2
0.0244	275.73	2.6
0.0454	277.26	4.3
0.0556	277.45	4.9
0.0654	277.37	5.4
0.0900	276.90	6.1
0.1299	276.21	6.3
0.1800	275.14	6.2
0.1881	275.02	6.1
	$\text{H}_{\text{II}}\text{L}_1 = \text{L}_2$	
0.0556	277.55	101.3
0.0556	277.50	26.3

composition of aqueous solution is given with one-to-one correspondence of each mixture prepared initially.

The stoichiometric solution giving a maximum temperature was supplied until the gas-phase disappeared, and then the univariant two-phase coexistence state was established by the same method. Finally, we can obtain four kinds of phase-equilibrium curves.

## Results and Discussion

**Stability Boundaries for THF Hydrate System in the Low-Pressure Region.** Four univariant curves below atmospheric pressure are shown in Figure 1. The symbols H<sub>II</sub>, S, L, and G stand for s-II THF hydrate, solid (ice Ih), aqueous solution, and gas phases, respectively. The subscript 1 means that the THF composition is lower than the stoichiometric ratio of s-II THF hydrate, and 2 means a composition greater than the stoichiometric ratio. The solid squares and open circles stand for experimental data of (H<sub>II</sub>(L<sub>1</sub> or L<sub>2</sub>)G) and (S<sub>1</sub>(ice Ih)L<sub>1</sub>G) obtained in the present study, respectively. The solid circles are also experimental data of univariant (H<sub>II</sub>L<sub>1</sub> = L<sub>2</sub> at  $x_{\text{THF}} = 0.0556$ ). The symbol  $x_{\text{THF}}$  stands for the equilibrium THF mole fraction

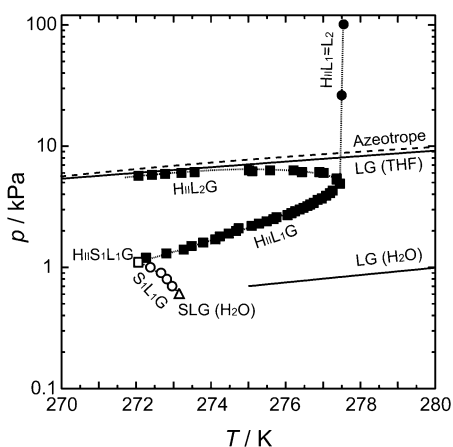


**Figure 1.** Phase equilibria for THF + water system below atmospheric pressure. ●, two-phase equilibrium point (H<sub>II</sub>L<sub>1</sub> = L<sub>2</sub> at  $x_{\text{THF}} = 0.0556$ ); ■, three-phase equilibrium point (H<sub>II</sub>(L<sub>1</sub> or L<sub>2</sub>)G); □, four-phase equilibrium point (H<sub>II</sub>S<sub>1</sub>L<sub>1</sub>G); ○, three-phase equilibrium point (S<sub>1</sub>L<sub>1</sub>G); △, three-phase equilibrium point of pure water (SLG); solid lines, calculated saturated vapor-pressure of pure THF and water;<sup>12</sup> dashed line, azeotropic locus estimated by PRSV EOS.<sup>15,16</sup>

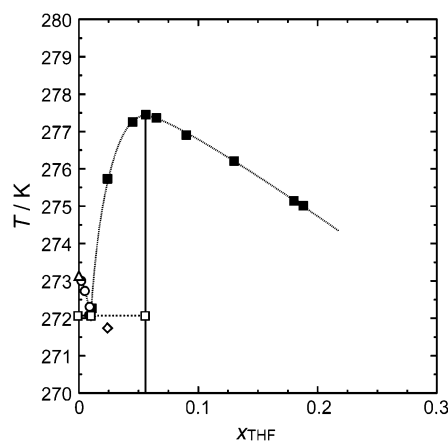


**Figure 2.** Temperature–composition projection for THF + water system (not isobaric condition). ■, three-phase equilibrium point (H<sub>II</sub>(L<sub>1</sub> or L<sub>2</sub>)G); □, four-phase equilibrium point (H<sub>II</sub>S<sub>1</sub>L<sub>1</sub>G); ○, three-phase equilibrium point (S<sub>1</sub>(ice Ih)L<sub>1</sub>G); △, three-phase equilibrium point of pure water (SLG); ●, three-phase equilibrium point (H<sub>II</sub>S<sub>1</sub>L<sub>1</sub>) at atmospheric pressure;<sup>8</sup> ◆, three-phase equilibrium point (H<sub>II</sub>S<sub>1</sub>L<sub>1</sub>) at atmospheric pressure;<sup>17</sup> ◇, three-phase equilibrium point (H<sub>II</sub>S<sub>1</sub>L<sub>1</sub>) at atmospheric pressure;<sup>18</sup> solid line, stoichiometric composition of s-II THF hydrate.

of the aqueous solution. The saturated vapor pressure of pure THF and pure water is calculated from Antoine-type equation.<sup>12</sup> The gas–liquid equilibrium curve for THF + water system shows an azeotrope below atmospheric pressure as the conditions of the present study.<sup>13,14</sup> The azeotropic locus was estimated by the Peng–Robinson equation of state modified by Stryjek and Vera (PRSV EOS).<sup>15,16</sup> The parameters of PRSV EOS used in the present study were reported in ref 15. An invariant point, where three phase-equilibrium curves of (H<sub>II</sub>L<sub>1</sub>G), (H<sub>II</sub>L<sub>2</sub>G), and (H<sub>II</sub>L<sub>1</sub> = L<sub>2</sub>) converge, is located at  $T = 277.45 \pm 0.02$  K and  $p = 4.9 \pm 0.1$  kPa.

Three three-phase equilibrium curves exist between the saturated vapor-pressure lines of THF and water. The (H<sub>II</sub>L<sub>1</sub>G) curve leads to the quadruple point of (H<sub>II</sub>S<sub>1</sub>L<sub>1</sub>G) (the open square in Figure 1). This quadruple point exists at  $T = 272.06 \pm 0.02$  K,  $p = 1.1 \pm 0.1$  kPa, and  $x_{\text{THF}} = 0.0106 \pm 0.0002$ . As extrapolating the (H<sub>II</sub>L<sub>2</sub>G) curve toward the lower temperature region, the curve reaches another quadruple point of (H<sub>II</sub>S<sub>2</sub>L<sub>2</sub>G). The (S<sub>1</sub>L<sub>1</sub>G) curve leads to the triple point of pure water (open triangle in Figure 1) from the quadruple point of (H<sub>II</sub>S<sub>1</sub>L<sub>1</sub>G). The univariant curve of two-phase equilibria (H<sub>II</sub>L<sub>1</sub> = L<sub>2</sub>), which originates from the maximum temperature point, shows an almost perpendicular slope in the region of the present study. The equilibrium temperature at atmospheric pressure shows good agreement with the literature data for the dissociation temperature.<sup>8–11</sup>

The equilibrium data obtained from different mixtures in the present study are shown in Figure 2 (not isobaric condition) and are listed in Table 1. The three-phase equilibrium point (H<sub>II</sub>S<sub>1</sub>L<sub>1</sub>) at atmospheric pressure is reported in ref 8, ref 17, and ref 18. They are also plotted in Figure 2 by solid circle, solid rhombus, and open rhombus, respectively. The solid circle and rhombus are hidden by the open square that exists at  $T = 272.06$  K and  $x_{\text{THF}} = 0.0106$  in Figure 2. The temperature–composition relation of our (H<sub>II</sub>S<sub>1</sub>L<sub>1</sub>G) data (open square in Figure 2) agrees well with that of ref 17 (the discrepancy is 0.01 K in temperature and less than 0.001 in mole fraction). The temperature of another three-phase equilibrium point (H<sub>II</sub>S<sub>1</sub>S<sub>2</sub>) at atmospheric pressure is about 164.14 K.<sup>18</sup> The symbol S<sub>2</sub> stands for the solid phase of THF. At the

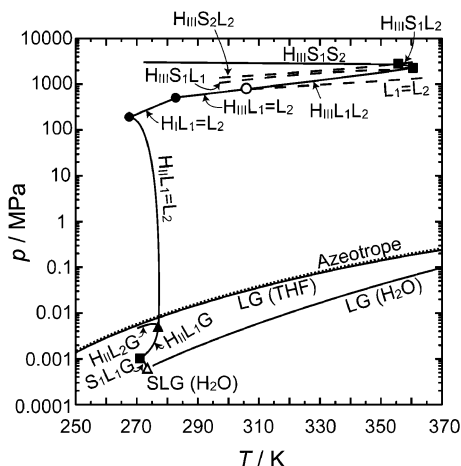


**Figure 3.** Schematic diagram of pressure–temperature projection for THF + water system.  $\Delta$ , triple point of pure water;  $\blacksquare$ , quadruple point;  $\blacktriangle$ , maximum temperature point;  $\bullet$ , hydrate structural transition point;  $\circ$ , liquid–liquid separation point.

maximum temperature (invariant point in Figure 1), congruent melting occurs and the equilibrium composition of the aqueous solution is equal to the stoichiometric composition of the s-II THF hydrate. In the present study, the liquid–liquid separation reported in ref 18 was not confirmed.

**Summary of Phase Behavior for THF + Water System.** The phase behavior of THF + water system obtained from the present results and previous works<sup>6,7</sup> is summarized in a schematic pressure–temperature projection shown in Figure 3. The gas–liquid equilibrium having an azeotropic point is laid at low pressure. In the low-pressure region, two three-phase equilibrium curves of ( $H_{II}L_1G$ ) and ( $S_1L_1G$ ) converge at the quadruple point of ( $H_{II}S_1L_1G$ ),  $T = 272.06$  K,  $p = 1.1$  kPa, and  $x_{THF} = 0.0106$ . Three characteristic phase-equilibrium curves (two three-phase coexistence curves of ( $H_{II}L_1G$ ) and ( $H_{II}L_2G$ ) and one univariant two-phase coexistence curve of ( $H_{II}L_1 = L_2$ )) converge at the invariant point,  $T = 277.45$  K and  $p = 4.9$  kPa under the stoichiometric composition (THF mole fraction is 0.0556). The ( $H_{II}L_1 = L_2$ ) turns toward the hydrate structural transition point (s-II to structure-I (s-I)) of about  $T = 268$  K and  $p = 0.2$  GPa.<sup>6,7</sup> The ( $H_{II}L_1 = L_2$ ) curve leads to the next transition point (s-I to another hydrate structure (s-III)), which exists at about  $T = 283$  K and  $p = 0.5$  GPa.<sup>7</sup> The symbol  $H_I$  stands for the s-I THF hydrate phase. It is reported that the hydration number of s-III is 5.<sup>7</sup> The ( $H_{III}L_1 = L_2$ ) curve, where  $H_{III}$  stands for s-III THF hydrate phase, divides into two curves. One is the ( $H_{III}L_1L_2$ ) and the other is the liquid–liquid critical locus ( $L_1 = L_2$ ). The ( $H_{III}L_1L_2$ ) curve intersects with the melting curve of ice VII, and there is the four-phase coexistence point of ( $H_{III}S_1L_1L_2$ ) near the cross point. The symbol  $S_1$  stands for ice VII phase. The three-phase equilibrium curves (( $H_{III}S_1L_1$ ), ( $H_{III}S_1L_2$ ), and ( $S_1L_1L_2$ )) originate from ( $H_{III}S_1L_1L_2$ ). The ( $H_{III}S_1L_2$ ) curve leads to the next quadruple point of ( $H_{III}S_1S_2L_2$ ), where  $S_2$  stands for pure solid THF phase. At this point, the ( $H_{III}S_1L_2$ ) curve divides into three three-phase equilibrium curves of ( $H_{III}S_1S_2$ ), ( $H_{III}S_2L_2$ ), and ( $S_1S_2L_2$ ).

## Conclusion

The phase equilibria for the tetrahydrofuran + water system were investigated below atmospheric pressure from  $T = 272$  K to 278 K. Two three-phase coexistence curves and one univariant curve converge at the invariant  $T =$

$277.45 \pm 0.02$  K and  $p = 4.9 \pm 0.1$  kPa in which the tetrahydrofuran composition is equal to the stoichiometric ratio of s-II THF hydrate. The THF hydrate cannot coexist with a gas phase beyond  $T = 277.45$  K. The four-phase (s-II hydrate + aqueous solution + ice Ih + gas) equilibrium point exists at  $T = 272.06 \pm 0.02$  K,  $p = 1.1 \pm 0.1$  kPa, and equilibrium tetrahydrofuran mole fraction of aqueous solution is  $0.0106 \pm 0.0002$ .

## Acknowledgment

The authors are grateful to the Division of Chemical Engineering, Graduate School of Engineering Science, Osaka University for the scientific support by “Gas-Hydrate Analyzing System (GHAS)”. T.M. expresses his special thanks for the center of excellence (21COE) program “Creation of Integrated EcoChemistry of Osaka University”.

## Literature Cited

- (1) Florusse, L. J.; Peters, C. J.; Schoonman, J.; Hester, K. C.; Koh, C. A.; Dec, S. F.; Marsh, K. N.; Sloan, E. D. Stable low-pressure hydrogen clusters stored in a binary clathrate hydrate. *Science* **2004**, *306*, 469–471.
- (2) Lee, H.; Lee, J.-W.; Kim, D. Y.; Park, J.; Seo, Y.-T.; Zeng, H.; Moudrakovski, I. L.; Ratcliffe, C. I.; Ripmeester, J. A. Tuning clathrate hydrates for hydrogen storage. *Nature* **2005**, *434*, 743–746.
- (3) Dyadin, Yu. A.; Bondaryuk, I. V.; Zhurko, F. V. Clathrate hydrates at high pressures. In *Inclusion Compounds, Vol. 5, Inorganic and Physical Aspects of Inclusion*; Atwood, J. L., Davies, J. E. D., MacNicol, D. D., Eds.; Oxford University Press: Oxford, 1991; pp 230–234.
- (4) Hawkins, R. E.; Davidson, D. W. Dielectric relaxation in the clathrate hydrates of some cyclic ethers. *J. Phys. Chem.* **1966**, *70*, 1889–1894.
- (5) Gough, S. R.; Davidson, D. W. Composition of tetrahydrofuran hydrate and the effect of pressure on the decomposition. *Can. J. Chem.* **1971**, *49*, 2691–2699.
- (6) Dyadin, Yu. A.; Kuznetsov, P. N.; Yakovlev, I. I.; Pyrinova, A. V. The system water–tetrahydrofuran in the crystallization region at pressures up to 9 kbar. *Dokl. Chem.* **1973**, *208*, 9–12.
- (7) Manakov, A. Yu.; Goryainov, S. V.; Kurnosov, A. V.; Likhacheva, A. Yu.; Dyadin, Yu. A.; Larionov, E. G. Clathrate nature of the high-pressure tetrahydrofuran hydrate phase and some new data on the phase diagram of the tetrahydrofuran–water system at pressures. *J. Phys. Chem. B* **2003**, *107*, 7861–7866.
- (8) Erva, J. The hydrates of tetrahydrofuran. *Suomen Kemistilehti B* **1956**, *29B*, 183.
- (9) Yamamuro, O.; Oguni, M.; Matsuo, T.; Suga, H. Calorimetric study of pure and KOH-doped tetrahydrofuran clathrate hydrate. *J. Phys. Chem. Solids* **1988**, *49*, 425–434.
- (10) Sloan, E. D., Jr. *Clathrate Hydrate of Natural Gases*, 2nd ed.; Marcel Dekker: New York, 1997.
- (11) Leaist, D. G.; Murray, J. J.; Post, M. L.; Davidson, D. W. Enthalpies of decomposition and heat capacities of ethylene oxide and tetrahydrofuran and hydrates. *J. Phys. Chem.* **1982**, *86*, 4175–4178.
- (12) Reid, R. C.; Prausnitz, J. M.; Poling, B. E. *The Properties of Gases and Liquids*, 4th ed.; McGraw-Hill: New York, 1986.
- (13) Matouš, J.; Novák, J. P.; Obr, J.; Pick, J. Phase equilibria in the system tetrahydrofuran (1)–Water (2). *Collect. Czech. Chem. Commun.* **1972**, *37*, 2653–2663.
- (14) Chen, S.-F.; Chen, Y.-P.; Tang, M. Vapor–liquid equilibrium calculations of azeotropic mixtures using the Peng–Robinson equation of state and various mixing rules. *J. Chem. Eng. Jpn.* **1994**, *27* (4), 512–516.
- (15) Stryjek, R.; Vera, J. H. PRSV: An improved Peng–Robinson equation of state for pure compounds and mixtures. *Can. J. Chem. Eng.* **1986**, *64*, 323–333.
- (16) Stryjek, R.; Vera, J. H. prsv—an improved Peng–Robinson equation of state with new mixing rules for strongly nonideal mixtures. *Can. J. Chem. Eng.* **1986**, *64*, 334–340.
- (17) Otake, K.; Tsuji, T.; Sato, I.; Akiya, T.; Sako, T.; Hongo, M. A proposal of a new technique for the density measurements of solids. *Fluid Phase Equilib.* **2000**, *171*, 175–179.
- (18) Ross, J.-C.; Carbonnel, L. The binary system water–tetrahydrofuran. *C. R. Acad. Sci. Paris* **1971**, *11* (22), C15–18.

Received for review July 11, 2005. Accepted September 7, 2005.

JE0502694